Concurrent Transmission and Multiuser Detection of LoRa Signals

The Khai Nguyen, Ha H. Nguyen, *Senior Member, IEEE*, and Ebrahim Bedeer, *Member, IEEE*

***Abstract*—This article investigates a new model to improve the scalability of low-power long-range (LoRa) networks by allowing a group of multiple end devices (EDs) to communicate with multiple multi-antenna gateways simultaneously (i.e., in the same time slot) on the same frequency band and using the same spreading factor. The maximum-likelihood (ML) decision rule is first derived for noncoherent detection of information bits transmitted by multiple devices in a group. To overcome the high complexity of the ML detection, we propose a suboptimal two-stage detection algorithm to balance the computational complexity and error performance. In the first stage, we identify transmitted chirps (without knowing which EDs transmit them). In the second stage, we determine the EDs that transmit the specific chirps identified from the first stage. To improve the detection performance in the second stage, we also optimize the transmit powers of EDs to minimize the similarity, measured by the Jaccard coefficient, between the received powers of any pair of EDs in the same group. As the power control optimization problem is nonconvex, we use concepts from successive convex approximation to transform it to an approximate convex optimization problem that can be solved iteratively and guaranteed to reach a suboptimal solution. Simulation results demonstrate and justify the tradeoff between transmit power penalties and network scalability of the proposed LoRa network model. In particular, by grouping two or three EDs in each group for concurrent transmission, the uplink capacity of the proposed network can be doubled or tripled over that of a conventional LoRa network, albeit at the expense of additional 3.0 or 4.7 dB transmit power.**

***Index Terms*—Chirp-spread spectrum modulation, Internet-of-Things, LoRa, LoRaWAN, multiuser detection (MUD), noncoherent detection, power control.**

I. Introduction

TECHNICAL advances and applications in the Internet of Things (IoT) domain continue to evolve in recent years in order to support communications and connectivity of billions of end devices (EDs) worldwide [1]. In many IoT applications, EDs need to communicate over distances of tens of kilometers with very low power consumption while being served by a few gateways (GWs). To satisfy such large coverage and low power consumption requirements, low-power wide-area networks (LPWANs) have been designed and deployed. Low-power long-range (LoRa) is one of the leading LPWAN technologies and is based on chirp spread spectrum (CSS), commonly refereed to in the literature as LoRa modulation in the PHY layer, and LoRaWAN protocol in the medium-access control (MAC) layer [2].

In the PHY layer, LoRa modulation can be configured with three different bandwidths of 125, 250, and 500 kHz, as well as six different spreading factor (SF) values, from 7 to 12. Using a higher SF increases the coverage range, but at the expense of a lower data rate [3]. In the MAC layer, the LoRaWAN protocol adopts pure ALOHA due to its simplicity and little communication overhead. However, pure ALOHA has its own shortcomings, the most critical of which is that a maximum duty cycle is often imposed on the transmitting devices to reduce the collision probability,[1] which also limits the scalability of LoRa networks [4].

In the uplink transmission of a typical LoRa network, single-antenna EDs communicate with a number of single-antenna GWs. Then, GWs forward the received packets to the LoRa network server (LNS) along with the received signal strength indicator (RSSI) of each packet and optional time stamps. In the downlink transmission, the LNS communicates with a given ED through the GW with the highest RSSI.

Most research works on LoRa modulation are concerned with communication between a single ED and multiple GWs, where both the ED and GWs are equipped with a single antenna [5], [6], [7], [8], [9], [11], [12]. For example, Elshabrawy and Robert [7] derived tight closed-form approximations for the bit error rate (BER) of the conventional LoRa modulation in both additive white Gaussian noise (AWGN) and Rayleigh fading channels. There are various improvements made to the basic LoRa modulation in order to increase its data rates. The interleaved-chirp spreading LoRa (ICS-LoRa) presented in [10] improves the data rates by using interleaved up chirps along with the up chirps. Hanif and Nguyen [8] presented another rate-improving method by adding a down chirp and its cyclic shifts to the signal set. Such a scheme is called slope-shift keying LoRa (SSK-LoRa). The authors also derived tight approximations for the BER and symbol error rate (SER) for noncoherent detection in Rayleigh fading channels. On the other hand, Nguyen *et al.* [9], Bomfin *et al.* [11], and Azim *et al.* [12] proposed to increase the data rates by embedding extra information bits in the phases of LoRa signals. It is pointed out, however, that embedding extra information bits in the phases requires the use of a more complicated coherent receiver, which must have

Manuscript received 15 March 2022; revised 3 July 2022 and 27 July 2022; accepted 29 August 2022. Date of publication 6 September 2022; date of current version 22 December 2022. This work was supported by the NSERC/Cisco Industrial Research Chair in Low-Power Wireless Access for Sensor Networks. *(Corresponding author: Ha H. Nguyen.)*

The authors are with the Department of Electrical and Computer Engineering, University of Saskatchewan, Saskatoon, SK S7N5A9, Canada (e-mail: khai.nguyen@usask.ca; ha.nguyen@usask.ca; e.bedeer@usask.ca).

Digital Object Identifier 10.1109/JIOT.2022.3204517

[1]For example, the maximum duty cycle in LoRaWAN is 1%.

the ability to estimate the channel state information (CSI). Another more flexible and advanced scheme is proposed in [5] and [6] and called frequency-shift CSS with index modulation (FSCSS-IM), which can offer much higher data rates than the conventional LoRa modulation. The higher data rates of FSCSS-IM are achieved without the need to increase the transmission bandwidth, but at the cost of a slight deterioration of the BER. The authors also proposed a low-complexity near-optimal noncoherent detection algorithm whose performance approaches its counterpart of the coherent detection. More recently, by extending the framework of FSCSS-IM in [5] and [6] to the quadrature dimension, Baruffa and Luca [13] proposed a scheme called quadrature chirp index modulation (QCIM). They also analyzed the BER performance of QCIM and compared it with other LoRa-based schemes.

There are only a few works on LoRa modulation that consider signal transmission from a single ED to GWs equipped with *multiple antennas* [14], [15]. In particular, Nguyen *et al.* [14] investigated performance improvement of the conventional LoRa modulation when multiple antennas are used at the GWs. They derived a BER expression for noncoherent detection in Rayleigh fading channels and proposed an iterative semi-coherent detection technique, whose performance is shown to approach that of the coherent detection without spending extra resources to estimate the channels.

The works in [16], [17], [18], [19], [20], and [21] investigated the scalability of LoRa modulation in the downlink transmission from a single-antenna GW to multiple EDs. In particular, Tesfay *et al.* [16] developed a power-domain nonorthogonal multiple access (PD-NOMA) approach in order to increase the number of EDs that can be served in the downlink transmission of an LoRa network. They demonstrated that by exploiting the spread spectrum property of LoRa modulation, the use of successive interference cancelation, which is common in NOMA, is not needed at EDs, and hence, maintaining their low complexity implementation. Similar to the methods in [9], [11], and [12], the method in [16] also requires CSI, which is challenging to obtain and not readily available in practical LoRa networks. Beltramelli *et al.* [17] evaluated the performance of ALOHA, slotted-ALOHA, and nonpersistent carrier-sense multiple access (CSMA) when used with LoRa modulation, and showed the tradeoff among various random multiple access techniques and parameters of LoRa modulation, such as SF, and the number of EDs and coverage area. In particular, Beltramelli *et al.* [17] showed that slotted-ALOHA has lower energy efficiency when the density of EDs in the LoRa network decreases. Furthermore, the performance of CSMA degrades at higher SFs.

Against the existing literature discussed above, in this article, we propose and investigate a new system model to improve the uplink scalability of LoRa networks by allowing concurrent transmission (in the same time slot) of multiple EDs to multiple multiantenna GWs using the same SF and over the same frequency band. In a nutshell, our system design embraces collision rather than suffering from it. For the proposed system to work, the most important task is to develop a detection algorithm that can jointly detect the information simultaneously (concurrently) transmitted by multiple EDs, an approach known as multiuser detection (MUD).

MUD is a well-researched topic and relevant in various digital communication systems, including satellite communications, digital television, magnetic recording, and wireless communications [22]. While the main principle of MUD is to jointly detect mutually interfering signals, detailed approaches are different and depend on the type and property of the interfering signals. For example, in code-division multiple-access (CDMA) systems, signals from multiple users are distinguished by the so-called signature sequences (waveforms). Due to the need to accommodate more and more users in a given time-bandwidth product [22], users are forced to use correlated (instead of orthogonal) signature sequences, causing inter-user interference in the received signal. The optimal maximum-likelihood (ML) detector can be implemented using the Viterbi algorithm, but its computational complexity is exponential in the number of users [23]. On the other hand, popular suboptimal MUD detectors include the decorrelating detector, minimum mean-square error (MMSE) linear detector, decision-feedback detector, and multistage detector [22], [24], [25]. All these optimal and suboptimal detectors developed for CDMA systems operate based on the matched filters' outputs and the correlation matrix of the signature sequences.

In contrast, in the proposed LoRa network, the multiple EDs that are grouped and allowed to transmit concurrently are not distinguished by signature sequences, but rather by the inherent spread spectrum property of the chirps, and the use of a large number of antennas at the receiver. Therefore, although the principle is the same (jointly detecting the concurrently transmitted signals), our developments of both the optimal ML and suboptimal MUD algorithms are different and novel for the proposed LoRa network. Another very important point is that the MUD detection algorithms developed for the proposed LoRa network can operate without CSI, i.e., noncoherently (whereas the MUD detection approaches developed for CDMA systems are mostly coherent detection, i.e., they require the CSI). To elaborate further, our contributions are summarized in the following.

1) We derive the noncoherent ML MUD of LoRa signals when multiple EDs are grouped for concurrent transmission to multiple multi-antenna GWs using the same SF and over the same bandwidth.
2) To overcome the high complexity of the ML detection, we exploit the unique structure of LoRa signals and develop a novel two-stage suboptimal detection algorithm to balance the computational complexity and detection performance. In particular, in the first stage, we develop a method to identify the transmitted chirps without knowing which EDs transmit the identified chirps. Detection of the chirp transmitted by each ED in the group is then carried out in the second stage (based on the information obtained in the first stage).
3) To improve the detection performance of the second stage, we optimize the transmit powers of EDs in each group to reduce the similarity, measured by the Jaccard coefficient, between the received powers of any pair

of EDs in the group. We show that the power control optimization problem is nonconvex, and hence, challenging to solve. We apply concepts from successive convex approximation to transform the nonconvex problem to an approximate convex one that can be solved iteratively and guaranteed to reach a suboptimal solution.

4) We provide extensive simulation results to demonstrate the merits of our proposed system model, the importance of power control, and the effectiveness of the two-stage suboptimal detection algorithm.

The remainder of this article is organized as follows. Section II introduces the system model. Section III derives the noncoherent ML MUD rule. The proposed two-stage suboptimal detection algorithm is presented in Section IV. The power control optimization problem is formulated and solved in Section V. Simulation results are provided in Section VI. Section VII concludes this article.

II. System Model

We consider the uplink transmission of an LoRa network in which single-antenna EDs communicate by means of CSS, or LoRa modulation with L GWs, each equipped with N_t antennas. Different from a conventional LoRa network, here N_u EDs are grouped together and are allowed to transmit simultaneously (i.e., in the same time slot) using the same frequency band and SF. Thus, compared to the conventional LoRa network in which no more than one ED can transmit in the same time slot over the same frequency band and using the same SF, the considered network can theoretically accommodate N_u times more devices in the same service area.

Let W and T_{sym} denote, respectively, the bandwidth and symbol duration of LoRa modulation. Then with the sampling period of $T_s = 1/W$, the number of samples in each LoRa symbol (i.e., chirp) is given as $M = T_{\text{sym}}/T_s = 2^{\text{SF}}$, where $\text{SF} \in \{7, 8, \ldots, 12\}$ is the SF, which is also the number of information bits that can be carried by one LoRa chirp. The basic baseband up chirp is made up of the following M time samples [8]:

$$x_0[n] = \exp\left\{j2\pi\left(\frac{n^2}{2M} - \frac{n}{2}\right)\right\},\ n = 0, 1 \ldots, M-1. \quad (1)$$

From this basic chirp, a set of M orthogonal chirps can be generated as follows:

$$x_m[n] = x_0[n+m],\ m = 0, 1 \ldots, M. \quad (2)$$

By allowing N_u EDs in each group to transmit simultaneously in the same frequency band and using the same SF, the $N_t \times 1$ received signal vector at the ℓth GW is given as follows:

$$\boldsymbol{y}_\ell[n] = \sum_{g=1}^{N_u} \boldsymbol{h}_{g,\ell}\sqrt{p_g}x_{m_g}[n] + \boldsymbol{w}_\ell[n] \quad (3)$$

where p_g denotes the transmit power of the gth ED, $g = 1, \ldots, N_u$, $x_{m_g}[n]$ is the chirp transmitted by the gth ED (i.e., the transmitted symbol is m_g, where $m_g \in \{0, 1, \ldots, M-1\}$), $\boldsymbol{w}_\ell[n] \sim \mathcal{CN}(0, \sigma^2\mathbf{I}_{N_t})$ is the vector of AWGN samples, and $\boldsymbol{h}_{g,\ell} \sim \mathcal{CN}(0, \beta_{g,\ell}\mathbf{I}_{N_t})$ is the vector of N_t uncorrelated Rayleigh fading channel gains between the gth ED and the ℓth GW, and $\beta_{g,\ell}$ represents the large-scale fading. The channel is assumed to stay constant within a coherence time of $T_c \gg T_{\text{sym}}$.

Allowing N_u EDs in each group to share the same bandwidth and SF causes inter-device interference, which needs to be properly handled at the network server. Suppressing the inter-device interference can be effectively done with coherent detection and by leveraging the large number of antennas at the GWs in order to achieve the asymptotic orthogonality property of the wireless channels among different EDs. Unfortunately, coherent detection requires extra time/frequency and processing resources for explicit channel estimation. Moreover, in order to have good channel estimation quality, the pilot power needs to be relatively high as compared to the noise level, which can be challenging in LoRa networks since EDs are typically battery operated and are expected to last for several years. Therefore, the main objective of this article is to develop *noncoherent* detection algorithms to recover the information bits transmitted simultaneously from multiple EDs in each group. The proposed detection algorithms take advantage of the large number of antennas at each GW and are presented in detail in the next sections.

III. Noncoherent Maximum-Likelihood Detection

With sufficient antenna spacing at each GW, it is reasonable to assume that the channels from an ED to the N_t antennas of a given GW are independent while experiencing the same large-scale fading. Under such an assumption, it is convenient to drop the antenna index in the following analysis. Specifically, the received signal at an arbitrary antenna of the ℓth GW is given as

$$y_\ell[n] = \sum_{g=1}^{N_u} h_{g,\ell}\sqrt{p_g}x_{m_g}[n] + w_\ell[n]. \quad (4)$$

The first step in detecting LoRa signals is to perform dechirping, i.e., multiplying the received signal at a given antenna with the conjugate of the basic chirp. Accordingly, the dechirped signal corresponding to an arbitrary antenna is given as follows [26]:

$$\begin{aligned} z_\ell[n] &= y_\ell[n]x_0^*[n] \\ &= \left[\sum_{g=1}^{N_u} h_{g,\ell}\sqrt{p_g}\exp\left\{j2\pi\left(\frac{(n+m_g)^2}{2M} - \frac{n+m_g}{2}\right)\right\} + w_\ell[n]\right] \\ &\quad \times \exp\left\{-j2\pi\left(\frac{n^2}{2M} - \frac{n}{2}\right)\right\} \\ &= \sum_{g=1}^{N_u} \underbrace{h_{g,\ell}\sqrt{p_g}\exp\left\{j2\pi\left(\frac{m_g^2}{2M} - \frac{m_g}{2}\right)\right\}}_{\text{constant gain}} \\ &\quad \times \underbrace{\exp\left\{\frac{j2\pi m_g n}{M}\right\}}_{\text{linear phase}} + \hat{w}_\ell[n] \\ &= \sum_{g=1}^{N_u} \hat{h}_{g,\ell}\sqrt{p_g}\exp\left\{\frac{j2\pi m_g n}{M}\right\} + \hat{w}_\ell[n]. \end{aligned} \quad (5)$$

In (5), we define $\hat{h}_{g,\ell} = h_{g,\ell}\exp\{j2\pi([m_g^2/2M]-[m_g/2])\}$ and $\hat{w}_\ell[n] = w_\ell[n]x_0^*[n] \sim \mathcal{CN}(0,\sigma^2)$. Next, we apply the M-point discrete Fourier transform (DFT) on the set of M dechirped signal samples $z_\ell[n]$, $n = 0,\ldots,M-1$, and obtain

$$\begin{aligned} Z_\ell[k] &= \frac{1}{\sqrt{M}}\sum_{n=0}^{M-1} z_\ell[n]\exp\left\{\frac{-j2\pi nk}{M}\right\} \\ &= \frac{1}{\sqrt{M}}\sum_{g=1}^{N_u}\hat{h}_{g,\ell}\sqrt{p_g}\sum_{n=0}^{M-1}\exp\left\{\frac{j2\pi n(m_g-k)}{M}\right\} + W_\ell[k] \\ &= \sqrt{M}\sum_{g\in\mathcal{U}_k}\hat{h}_{g,\ell}\sqrt{p_g} + W_\ell[k], \quad k = 0,1,\ldots,M-1 \end{aligned} \tag{6}$$

where $\mathcal{U}_k = \{g|m_g = k\}$ is the set of all EDs in the group that transmit the kth chirp (corresponding to the kth frequency bin after the DFT). The last identity in (6) follows from the fact that the second sum in the line above equals to M when $m_g = k$ and zero when $m_g \neq k$.

Equation (6) gives the values across the M frequency bins corresponding to an arbitrary single antenna at the ℓth GW. Collecting these observations over the entire antenna array of the ℓth GW yields an $N_t \times 1$ vector for the kth frequency bin as

$$\boldsymbol{Z}_\ell[k] = \sqrt{M}\sum_{g\in\mathcal{U}_k}\hat{\boldsymbol{h}}_{g,\ell}\sqrt{p_g} + \boldsymbol{W}_\ell[k],\ k = 0,1,\ldots,M-1 \tag{7}$$

where $\hat{\boldsymbol{h}}_{g,\ell} \sim \mathcal{CN}(0,\beta_{g,\ell}\mathbf{I}_{N_t})$ since it is simply a phase-rotated version of $\boldsymbol{h}_{g,\ell}$. As a result, $\boldsymbol{Z}_\ell[k]$ is a vector of random variables with distribution $\boldsymbol{Z}_\ell[k] \sim \mathcal{CN}(0,(M\sum_{g\in\mathcal{U}_k}p_g\beta_{g,\ell} + \sigma^2)\mathbf{I}_{N_t})$.

Since noncoherent detection of LoRa signals is based on the received signal powers at different frequency bins, we define $r_{\ell,k} = \boldsymbol{Z}_\ell^H[k]\boldsymbol{Z}_\ell[k]$ as the total received power at the ℓth GW over the kth frequency bin, where $(\cdot)^H$ refers to the Hermitian operator. Collecting the signal powers in all M frequency bins, we define $\boldsymbol{r}_\ell = [r_{\ell,0}, r_{\ell,1},\ldots,r_{\ell,M-1}]^\top$. Also for convenience, we represent all the symbols transmitted by N_u EDs in a given group as $\boldsymbol{m} = [m_1, m_2,\ldots,m_{N_u}]$.

The development of the ML detection algorithm in this section exploits the large number of antennas at each GW. Specifically, as N_t tends to infinity, the per-antenna average power $(1/N_t)r_{\ell,k}$ at the ℓth GW over the kth frequency bin converges to a sum of average signal powers from the EDs transmitting the kth chirp, plus the noise power, i.e.,

$$\frac{1}{N_t}r_{\ell,k} \xrightarrow[N_t\to\infty]{\text{a.s}} M\sum_{g\in\mathcal{U}_k}\beta_{g,\ell}p_g + \sigma^2 \triangleq \rho_{\ell,k}. \tag{8}$$

It is noted that (8) is well-known in the massive multiple-input multiple-output (MIMO) literature as the *channel hardening property* [27] which is a consequence of uncorrelated Rayleigh fading channels over the multiple antennas at each GW. In fact, one can show that $r_{\ell,k} = \boldsymbol{Z}_\ell^H[k]\boldsymbol{Z}_\ell[k]$ is a Chi-square random variable with $2N_t$ degrees of freedom with the following probability density function:

$$f(r_{\ell,k}) = \frac{1}{(\rho_{\ell,k})^{N_t}(N_t-1)!}r_{\ell,k}^{N_t-1}\exp\left\{-\frac{r_{\ell,k}}{\rho_{\ell,k}}\right\}. \tag{9}$$

Using the fact that the power vectors $\{\boldsymbol{r}_\ell\}_{\ell=1}^L$ are statistically independent across the L GWs, the likelihood function of power vectors $\{\boldsymbol{r}_\ell\}_{\ell=1}^L$ conditioned on the transmitted symbols $\boldsymbol{m} = [m_1, m_2,\ldots,m_{N_u}]$ can be written as follows:

$$\begin{aligned} \mathfrak{L}(\boldsymbol{r}_1,\boldsymbol{r}_2,\ldots,\boldsymbol{r}_L|\boldsymbol{m}) &= \prod_{\ell=1}^{L}\prod_{k=0}^{M-1} f(r_{\ell,k}) \\ &= \prod_{\ell=1}^{L}\prod_{k=0}^{M-1}\frac{1}{(\rho_{\ell,k})^{N_t}(N_t-1)!}r_{\ell,k}^{N_t-1}\exp\left\{-\frac{r_{\ell,k}}{\rho_{\ell,k}}\right\} \end{aligned} \tag{10}$$

and the corresponding log-likelihood function is

$$\begin{aligned} \hat{\mathfrak{L}}(\boldsymbol{r}_1,\boldsymbol{r}_2,\ldots,\boldsymbol{r}_L|\boldsymbol{m}) &= \ln(\mathfrak{L}(\boldsymbol{r}_1,\boldsymbol{r}_2,\ldots,\boldsymbol{r}_L|\boldsymbol{m})) \\ &= LM\ln\left\{\frac{1}{(N_t-1)!}\right\} + \sum_{\ell=1}^{L}\sum_{k=0}^{M-1}\left(\ln\left(\frac{r_{\ell,k}^{N_t-1}}{\rho_{\ell,k}^{N_t}}\right) - \frac{r_{\ell,k}}{\rho_{\ell,k}}\right). \end{aligned} \tag{11}$$

It is pointed out that the dependence of the likelihood function (and log-likelihood function) on $\boldsymbol{m}$ is through the sets $\{\mathcal{U}_k\}_{k=1}^M$, which determine the values of $\rho_{\ell,k}$ as defined in (8).

Since $\ln(\cdot)$ is a monotonically increasing function and $LM\ln(1/(N_t-1)!)$ is a constant that is independent of the transmitted symbols, the noncoherent ML detection of the transmitted N_u-tuple can be expressed as follows:

$$\begin{aligned} \hat{\boldsymbol{m}} &= \underset{\boldsymbol{m}\in\mathcal{S}_0}{\text{argmax}}\quad \hat{\mathfrak{L}}(\boldsymbol{r}_1,\boldsymbol{r}_2,\ldots,\boldsymbol{r}_L|\boldsymbol{m}) \\ &= \underset{\boldsymbol{m}\in\mathcal{S}_0}{\text{argmax}}\quad \sum_{\ell=1}^{L}\sum_{k=0}^{M-1}\left(\ln\left(\frac{r_{\ell,k}^{N_t-1}}{\rho_{\ell,k}^{N_t}}\right) - \frac{r_{\ell,k}}{\rho_{\ell,k}}\right) \end{aligned} \tag{12}$$

where $\mathcal{S}_0$ denotes the set of all possible N_u-tuples.

While finding the optimal solution for the ML detection problem in (12) is conceptually simple, the exhaustive search over the set $\mathcal{S}_0$ requires a complexity in the order of M^{N_u}, which is clearly prohibitive for $M = 2^{\text{SF}}$ with $\text{SF} = \{7,8,\ldots,12\}$ used in practical LoRa networks. Hence, in the next section we shall present a suboptimal low-complexity detection algorithm. The key idea of our proposed suboptimal detection algorithm is to reduce the search space by exploiting the fact that, since we have at most N_u EDs in each group that can transmit at any given time, there will be *atmost* $N_u \ll M$ chirps transmitted in every symbol duration.

IV. Proposed Low-Complexity Detection Algorithm

As discussed earlier, the search space can be reduced by noting that for the simultaneous uplink transmission of N_u EDs in each group, where each ED can transmit one chirp out of M possible chirps, we will have at most $N_u \ll M$ chirps transmitted every symbol duration. However, it is possible that the same chirp is transmitted by more than one ED. Thus, the number of different transmitted chirps, denoted by i, that are transmitted by N_u EDs in each group satisfies $1 \le i \le N_u$. The proposed suboptimal detection algorithm solves the MUD problem in (12) by decoupling it into two subproblems that are solved in two stages. In the first stage, the algorithm identifies the i transmitted chirps ($1 \le i \le N_u \ll M$) out of the M possible chirps without knowing which EDs transmit which

identified chirps. In the second stage, the algorithm determines which EDs that transmit which chirps out of i chirps that are identified from the first stage. Clearly, the size of the search space in the second stage is i^{N_u}, which is much smaller than the size M^{N_u} of $\mathcal{S}_0$.

A. First Stage: Identifying the Transmitted Chirps

With noncoherent detection, identifying the transmitted chirps amounts to identifying the active frequency bins based on the powers calculated at all the GWs. As shown in (8), as the number of antennas N_t at each GW tends to infinity, the power $(1/N_t)r_{\ell,k}$ provided by the antenna array of the ℓth GW over the kth frequency bin converges to $\rho_{\ell,k}$. It follows that the sum of $(1/N_t)r_{\ell,k}$ over all the L GWs at the kth frequency bin approaches to:

$$\Upsilon[k] = \frac{1}{N_t}\sum_{\ell=1}^{L} r_{\ell,k} \xrightarrow[N_t\to\infty]{\text{a.s}} \sum_{\ell=1}^{L}\rho_{\ell,k} = \begin{cases} M\sum_{\ell=1}^{L}\sum_{g\in\mathcal{U}_k}\beta_{g,\ell}p_g + L\sigma^2, & \mathcal{U}_k \neq \emptyset \\ L\sigma^2, & \text{otherwise} \end{cases} \tag{13}$$

where $\mathcal{U}_k = \{g|m_g = k\}$ is the set of all EDs in each group that transmit the kth chirp.

The expression in (13) suggests that one can choose a power threshold of $L\sigma^2$ to detect whether the kth chirp was transmitted, i.e., whether the kth frequency bin is *active*. However, using such a threshold yields error-free detection only under the theoretical assumption of having an infinite number of antennas N_t at each GW. Under a practical situation of having a limited (although can be very large) number of antennas at each GW, a proper power threshold needs to be found. Specifically, the kth frequency bin is identified to be active or not by comparing $\Upsilon[k]$ with a certain power threshold P_{th} as follows:

$$\Upsilon[k] \underset{\text{inactive}}{\overset{\text{active}}{\gtrless}} P_{\text{th}}, \quad k = 0, 1, \ldots, M-1. \tag{14}$$

Finding the value of P_{th} is crucial to the successful identifications of the active frequency bins, and this is discussed in the rest of this section.

We showed in (9) that $r_{\ell,k}$ is a Chi-square distributed random variable with $2N_t$ degrees of freedom. For a large number of antennas at each GW, $r_{\ell,k}/N_t$ can be approximated as a Gaussian random variable with mean $\rho_{\ell,k}$ and variance $\rho_{\ell,k}^2/N_t$. Then, it follows that:

$$\Upsilon[k] \sim \mathcal{CN}\left(\sum_{\ell=1}^{L}\rho_{\ell,k}, \sum_{\ell=1}^{L}\rho_{\ell,k}^2/N_t\right). \tag{15}$$

Equation (15) reveals that the mean and variance of $\Upsilon[k]$ depend on whether the kth frequency bin is active or not. Furthermore, in case the kth frequency bin is active, it depends on the number of EDs in each group that transmit the kth chirp.

With the concurrent transmission of N_u EDs in each group in the same time slot, we know that there are at most $N_u \ll M$ transmitted chirps in every symbol duration, and hence, there are at most N_u active frequency bins. Therefore, for a given P_{th}, the decision rule to identify the active frequency bins is as follows.

1) If there are $i \leq N_u$ frequency bins having powers higher than P_{th}, all of the i frequency bins are identified as active.
2) If there are $i > N_u$ frequency bins having powers higher than P_{th}, only the N_u frequency bins with the highest powers are identified as active.

Using the above decision rule, we can find P_{th} to minimize the error probability (i.e., the false alarm probability), which is equivalent to maximizing the probability of detecting the active bins correctly.

Let N^+, $1 \leq N^+ \leq N_u$, denote the number of different chirps sent by N_u EDs in each group. Then, the events of correct identification of N^+ are as follows.

1) $N^+ = N_u$ chirps are transmitted, and $\Upsilon[k]$ on all the N_u true active frequency bins are above P_{th} and also greater than the powers on all other $M - N_u$ true inactive frequency bins (note that it is possible to have the measured power on a true inactive bin higher than P_{th}).
2) $N^+ = i < N_u$ chirps are transmitted, and $\Upsilon[k]$ on all the i true active frequency bins are above P_{th}, whereas the powers on all the $M - i$ inactive frequency bins are below P_{th}.

Then, the probability of correct identification of the N^+ active frequency bins can be calculated as follows:

$$P_{\text{correct}} = P\big(\text{correct}|N^+ = N_u\big)P\big(N^+ = N_u\big) + \sum_{i=1}^{N_u-1} P\big(\text{correct}|N^+ = i\big)P\big(N^+ = i\big). \tag{16}$$

The computation of each term in the above expression is as follows.

First, the case $N^+ = N_u$ means that the chirps sent by N_u EDs in each group are all different. In other words, the set $\mathcal{U}_k$ corresponding to each active frequency bin includes one ED only. Without loss of generality, we index the active frequency bins from $g = 1$ to $g = N_u$ and use the random variable Υ_g to denote the power calculated in each of these active frequency bins. It is noted that, while the actual powers calculated over active frequency bins are likely different in each symbol duration, all the active bins' powers have the same statistics and can be characterized by the random variable Υ_g. Specifically, it follows from (13) that $\Upsilon_g \sim f_{\Upsilon_g} = \mathcal{CN}(L\mu_g, L\sigma_g^2/N_t)$, where

$$\mu_g = \frac{1}{L}\sum_{\ell=1}^{L}\Big(M\beta_{g,\ell}p_g + \sigma^2\Big) \tag{17}$$

and

$$\sigma_g^2 = \frac{1}{L}\sum_{\ell=1}^{L}\Big(M\beta_{g,\ell}p_g + \sigma^2\Big)^2. \tag{18}$$

Likewise, we use the random variable $\Upsilon_{\bar{g}}$ to denote the power calculated in each of the remaining $M - N_u$ inactive frequency bins. Then, it follows from (13) that $\Upsilon_{\bar{g}}$ is a Chi-square distributed random variable with $2N_tL$ degrees of freedom.

Then, the probability $P(\text{correct}|N^+ = N_u)$ can be calculated as follows:

$$\begin{aligned}P\big(\text{correct}|N^+ = N_u\big) &= \sum_{g=1}^{N_u} \int_{P_{\text{th}}}^{\infty} \big[P(\text{inactive bin's power} < U_0)\big]^{M-N_u} \\ &\quad \times f_{\Upsilon_g}(g\text{th active bin's power} = U_0) \\ &\quad \times \prod_{q=1, q\neq g}^{N_u} P(q\text{th active bin's power} > U_0) dU_0. \quad (19)\end{aligned}$$

The probability that the gth active frequency bin's power is higher than U_0 is

$$\begin{aligned}P\big(g\text{th active bin}'s \text{ power} > U_0\big) &= P\big(\Upsilon_g > U_0\big) \\ &= \frac{1}{\sqrt{2\pi L\sigma_g^2/N_t}} \int_{U_0}^{\infty} \exp\left\{-\frac{(U_0 - L\mu_g)^2}{2L\sigma_g^2/N_t}\right\} dU_0 \\ &= \frac{1}{2} - \frac{1}{2}\text{erf}\left(\frac{U_0 - L\mu_g}{\sqrt{2L\sigma_g^2/N_t}}\right). \quad (20)\end{aligned}$$

On the other hand, the probability that the powers in $M - N_u$ inactive frequency bins are all below an arbitrary value U_0 is

$$\begin{aligned}&\big[P\big(\text{inactive bin}'s \text{ power} < U_0\big)\big]^{M-N_u} \\ &= \big[P\big(\Upsilon_{\tilde{g}} < U_0\big)\big]^{M-N_u} \\ &= \left(1 - \exp\left(-\frac{U_0}{\sigma^2}\right) \sum_{q=0}^{N_t L-1} \frac{1}{q!}\left(\frac{U_0}{\sigma^2}\right)^q\right)^{M-N_u}. \quad (21)\end{aligned}$$

Substituting (17), (18), (20), and (21) into (19) yields

$$\begin{aligned}P\big(\text{correct}|N^+ = N_u\big) &= \sum_{g=1}^{N_u} \frac{1}{\sqrt{2\pi L\sigma_g^2/N_t}} \int_{P_{\text{th}}}^{\infty} \exp\left\{-\frac{(U_0 - L\mu_g)^2}{2L\sigma_g^2/N_t}\right\} \\ &\quad \times \left(1 - \exp\left(-\frac{U_0}{\sigma^2}\right) \sum_{q=0}^{N_t L-1} \frac{1}{q!}\left(\frac{U_0}{\sigma^2}\right)^q\right)^{M-N_u} \\ &\quad \times \prod_{q=1, q\neq g}^{N_u} \left[\frac{1}{2} - \frac{1}{2}\text{erf}\left(\frac{U_0 - L\mu_g}{\sqrt{2L\sigma_q^2/N_t}}\right)\right] dU_0. \quad (22)\end{aligned}$$

Next, for the case $N^+ = i < N_u$, we have

$$\begin{aligned}P\big(\text{correct}|N^+ = i\big) &= \big[P\big(\text{inactive bin}'s \text{ power} < P_{\text{th}}\big)\big]^{M-i} \\ &\quad \times \prod_{q=1}^{i} P\big(q\text{th active bin}'s \text{ power} > P_{\text{th}}\big). \quad (23)\end{aligned}$$

Unlike the case $N^+ = N_u$ where each active frequency bin corresponds to only one ED and the mean and variance of the power variable Υ_g for each active frequency bin can be determined easily, the mean and variance of $\Upsilon[k]$ for each active frequency bin in the case $N^+ = i < N_u$ depend on how the N_u EDs in each group share these i active bins. Given the high complexity involved in obtaining an exact expression for $P(\text{correct}|N^+ = i)$, we seek a simpler lower bound. To this end, we identify the i smallest values of μ_g in (17) [or equivalently σ_g^2 in (18)] over $g = 1, \ldots, N_u$ and use them as the means and variances of power variables $\Upsilon[k]$ for the i active frequency bins. Doing so leads to the following lower bound of (23):

$$\begin{aligned}P\big(\text{correct}|N^+ = i\big) &\geq P^{(\text{LB})}\big(\text{correct}|N^+ = i\big) \\ &= \left(1 - \exp\left(-\frac{P_{\text{th}}}{\sigma^2}\right) \sum_{q=0}^{N_t L-1} \frac{1}{q!}\left(\frac{P_{\text{th}}}{\sigma^2}\right)^q\right)^{M-i} \\ &\quad \times \prod_{g\in\mathcal{S}_i} \left[\frac{1}{2} - \frac{1}{2}\text{erf}\left(\frac{P_{\text{th}} - L\mu_g}{\sqrt{2L\sigma_g^2/N_t}}\right)\right] \quad (24)\end{aligned}$$

where $\mathcal{S}_i$ denotes the set of i EDs giving the i lowest values of μ_g.

The only thing left to find the lower bound on the probability of correct identification in (16) is to calculate the probability of having i chirps transmitted by N_u EDs. It is given as follows:

$$P\big(N^+ = i\big) = \frac{C_i \binom{M}{i}}{M^{N_u}},\ i = 1, \ldots, N_u \quad (25)$$

where C_i is the total number of possible N_u-tuples given i chirps are transmitted. This quantity can be easily found in a recursive manner as outlined in Lemma 1 as follows.

Lemma 1: Given the identities of i transmitted chirps, the total number of possible N_u-tuples can be calculated as follows:

$$C_1 = 1 \quad (26a)$$

$$C_i = i^{N_u} - \sum_{k=1}^{i-1} C_k \binom{i}{k}. \quad (26b)$$

Proof: If all N_u EDs transmit the same chirp, then the number of possible N_u-tuples is obviously $C_1 = 1$. If there are two chirps transmitted, an ED transmits either one of these two chirps. As a result, the number of possible N_u-tuples is 2^{N_u}. By excluding the case that all EDs transmit the same chirp (either one of the two transmitted chirps), we have $C_2 = 2^{N_u} - 1 \times 2$. Similarly, when three chirps are transmitted, the number of candidate N_u-tuples is equal 3^{N_u}. By excluding the cases when all EDs transmit one or two chirps, we have $C_3 = 3^{N_u} - C_2 \times \binom{3}{2} - C_1 \times \binom{3}{1}$. Proceeding in the same way, one can show that the number of possible N_u-tuples when i chirps are transmitted can be calculated as in Lemma 1. ■

In summary, the probability of correct identification of the N^+ active frequency bins (which is equivalent to identifying the N^+ transmitted chirps) in (16) can be lower bounded as follows:

$$\begin{aligned}P_{\text{correct}}^{(\text{LB})} &= P\big(\text{correct}|N^+ = N_u\big)P\big(N^+ = N_u\big) \\ &\quad + \sum_{i=1}^{N_u-1} P^{(\text{LB})}\big(\text{correct}|N^+ = i\big)P\big(N^+ = i\big). \quad (27)\end{aligned}$$

Obviously, the error probability in identifying the transmitted chirps is upper bounded by

$$P_{\text{error}}^{(\text{UB})} = 1 - P_{\text{correct}}^{(\text{LB})}. \quad (28)$$

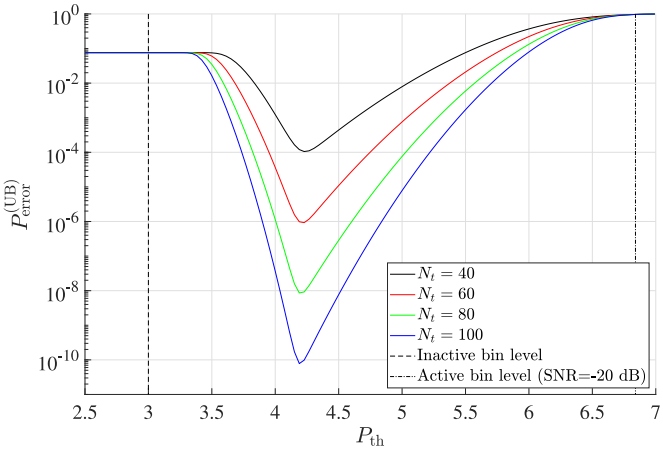

Fig. 1. Error probability of detecting active bins (i.e., transmitted chirps), SNR $= -20$ dB with five EDs in each group.

In Fig. 1, we plot $P_{\text{error}}^{(\text{UB})}$ versus P_{th} for different numbers of antennas at the GWs. As can be seen, $P_{\text{error}}^{(\text{UB})}$ is a unimodal function of P_{th}. Hence, the optimal value of P_{th} that minimizes the upper bound of the error probability in identifying the transmitted chirps can be easily found, for example by the Golden search.

B. Second Stage: Detection of Chirps Transmitted by the EDs

It can be seen from Lemma 1 that if the transmitted chirps have been identified, the total number of possible N_u-tuples is significantly smaller than that in the original problem in (12). For example, if $N_u = 5$, the number of possible N_u-tuples calculated according to Lemma 1 is $C_1 = 1$, $C_2 = 30$, $C_3 = 150$, $C_4 = 240$, and $C_5 = 120$, which are much smaller than M^5. Furthermore, the number of possible N_u-tuples in Lemma 1 is independent of M and only depends on the number of EDs in each group sharing the same frequency band and SF. It is clear that identifying the transmitted chirps plays a crucial role to reduce the complexity of the proposed detection algorithm.

After the active frequency bins have been identified from stage 1, the original candidate set $\mathcal{S}_0$ in (12) is replaced with a reduced set, denoted by $\mathcal{S}_d$, which contains all possible N_u-tuples constructed from the identified (active) frequency bins from stage 1. The ML MUD problem in (12) then becomes

$$\hat{\boldsymbol{m}} = \underset{\mathcal{S}_d}{\text{argmax}} \quad \sum_{\ell=1}^{L} \sum_{k=0}^{M-1} \left(\ln \left(\frac{r_{\ell,k}^{N_t-1}}{\rho_{\ell,k}^{N_t}} \right) - \frac{r_{\ell,k}}{\rho_{\ell,k}} \right). \tag{29}$$

The tradeoff for reducing the complexity from searching over $\mathcal{S}_0$ to searching over $\mathcal{S}_d$ is performance degradation since a mistake in the active bin identification in stage 1 may lead to error propagation and potentially remove the true transmitted N_u-tuple from the candidate set $\mathcal{S}_d$. However, from the simulation results, we will show that the performance gap between searching over the reduced set $\mathcal{S}_d$ and the original set $\mathcal{S}_0$ is small. Intuitively, when the active frequency bin identification in stage 1 is wrong, it means there are inactive frequency bins having powers higher than the active frequency bins' powers. In such a case, even the detection based on the original candidate set $\mathcal{S}_0$ will likely be wrong.

Even with the reduced candidate set $\mathcal{S}_d$, the detection in (29) can be made a little simpler. Specifically, it can observed from (29) that the contributions of the inactive frequency bins to the log-likelihood function are identical for all transmitted N_u-tuples in the reduced set, and hence, can be removed. This observation leads to the following simpler detection rule:

$$\hat{\boldsymbol{m}} = \underset{\mathcal{S}_d}{\text{argmax}} \quad \sum_{\ell=1}^{L} \sum_{k \in \mathcal{S}_+} \left(\ln \left(\frac{r_{\ell,k}^{N_t-1}}{\rho_{\ell,k}^{N_t}} \right) - \frac{r_{\ell,k}}{\rho_{\ell,k}} \right) \tag{30}$$

where $\mathcal{S}_+$ is the set of active frequency bins identified in Stage 1.

V. Power Control

Recall that the proposed suboptimal detection algorithm consists of two stages: stage 1 identifies active frequency bins without specifying associated EDs, whereas stage 2 detects the EDs associated with the active frequency bins identified in stage 1 by solving the simplified MUD problem in (30). It can be observed from (30) that the detection performance in stage 2 strongly depends on the difference in the received power levels of the transmitting EDs on the identified active frequency bins at the L GWs. More specifically, if the received powers of the EDs on the identified active frequency bins are dissimilar, it will be easier to detect these EDs. This observation suggests we can perform a suitable power control policy of the transmitting EDs to produce dissimilar received power levels at the L GWs, and hence improving the performance of the MUD in (30).

A. Power Control Problem Formulation

To develop a suitable power control problem, we denote the expected bin power of the gth ED, $g = 1, \ldots, N_u$, at the L GWs as the $L \times 1$ vector $\hat{\boldsymbol{\mu}}_g = [\mu_{g,1}, \mu_{g,2}, \ldots, \mu_{g,L}]^T$, where $\hat{\mu}_{g,\ell} = M\beta_{g,\ell}p_g + \sigma^2$ if only the gth ED transmits on the identified active bin. The objective of the proposed power control policy is to minimize the similarity of the expected bin power vectors among different EDs, i.e., $\hat{\boldsymbol{\mu}}_g$ and $\hat{\boldsymbol{\mu}}_{g'}$, for $g \neq g'$. A possible choice to measure the similarity between the two vectors $\hat{\boldsymbol{\mu}}_g$ and $\hat{\boldsymbol{\mu}}_{g'}$ is the Jaccard coefficient [28], defined as follows:

$$J_{g,g'} = \frac{\hat{\boldsymbol{\mu}}_g^T \hat{\boldsymbol{\mu}}_{g'}}{\|\hat{\boldsymbol{\mu}}_g\|^2 + \|\hat{\boldsymbol{\mu}}_{g'}\|^2 - \hat{\boldsymbol{\mu}}_g^T \hat{\boldsymbol{\mu}}_{g'}}, \quad g \neq g'. \tag{31}$$

It can be verified that $J_{g,g'}$ lies between 0 to 1, with the value of 1 representing the highest similarity and the value of 0 representing the lowest similarity between the two vectors.

The Jaccard coefficient defined in (31) measures the similarity between the expected bin powers of two EDs g and g', $g \neq g'$, across the L GWs. The definition of $\hat{\boldsymbol{\mu}}_g$ and $\hat{\boldsymbol{\mu}}_{g'}$ assumes that the two EDs g and g' transmit two different chirps. However, it is possible that two or more EDs transmit the same chirps, and if this scenario is not taken into account in the power control policy, errors may occur. This is because

the contribution to the received powers at the GWs from one ED can be too weak compared to that of the other ED, and the detector may not realize that there are two transmitting EDs on the same frequency bin. The Jaccard coefficient when two EDs transmit the same chirp can be defined as follows:

$$J^{(2)}_{g,g'} = \frac{\hat{\boldsymbol{\mu}}^T_{g,g'}\hat{\boldsymbol{\mu}}_{g'}}{\left\|\hat{\boldsymbol{\mu}}_{g,g'}\right\|^2 + \left\|\hat{\boldsymbol{\mu}}_{g'}\right\|^2 - \hat{\boldsymbol{\mu}}^T_{g,g'}\hat{\boldsymbol{\mu}}_{g'}} \tag{32}$$

where $\hat{\boldsymbol{\mu}}_{g,g'}$ is the expected bin power of when both the gth and g'th EDs transmit the same chirp at the L GWs. It is defined as $\hat{\boldsymbol{\mu}}_{g,g'} = [\mu_{g,g',1}, \mu_{g,g',2}, \ldots, \mu_{g,g',L}]^T$, $g \neq g'$, where $\hat{\mu}_{g,g',\ell} = M\beta_{g,\ell}p_g + M\beta_{g',\ell}p'_g + \sigma^2$.

Taking both $J_{g,g'}$ and $J^{(2)}_{g,g'}$ into account, the power control problem to improve the MUD performance in (30) is formally expressed as follows:

$$\begin{aligned}\mathcal{OP}_1 : \min_{p_g} \max_{g,g'} \ & \left\{J_{g,g'}, J^{(2)}_{g,g'}\right\} \\ \text{subject to} \ & 0 \le p_g \le p_{\max} \quad \forall g \qquad (33) \\ & \frac{1}{L\sigma^2}\sum_{\ell=1}^{L} M\beta_{g,\ell}p_g \ge \xi \quad \forall g \qquad (34)\end{aligned}$$

where the constraint in (33) ensures that the ED's transmit power does not exceed a certain power budget $p_{\max}$, and the constraint in (34) guarantees that the average received SNR exceeds a predefined threshold ξ.

The optimization problem $\mathcal{OP}_1$ is nonconvex because of the nonconvexity of $J_{g,g'}$ and $J^{(2)}_{g,g'}$. To facilitate obtaining a low-complexity suboptimal solution, it is more convenient to work with its equivalent epigraph form. After a change of variables, $\mathcal{OP}_1$ can be reformulated as follows:

$$\begin{aligned}\mathcal{OP}_2 : \max_{p_g,\lambda} \ & \lambda \\ \text{subject to} \ & (33), \ (34) \\ & J^{-1}_{g,g'} \ge \lambda \ \forall g < g' \qquad (35) \\ & \left(J^{(2)}_{g,g'}\right)^{-1} \ge \lambda \ \forall g < g'. \qquad (36)\end{aligned}$$

As can be seen in $\mathcal{OP}_2$, maximizing λ in the objective function will maximize the lower bound of $J^{-1}_{g,g'}$, $g < g'$. This is equivalent to minimizing the upper bound of $J_{g,g'}$, $g < g'$, which enforces $J_{g,g'}$ to reduce its value. Similarly, maximizing λ in the objective function also enforces $J^{(2)}_{g,g'}$ to reduce its value. Hence, by solving $\mathcal{OP}_2$, we can reduce the similarities among the transmit power vectors of EDs, which eventually helps to improve the detection performance.

It is pointed out that, because of the nonconvexity of the constraints in (35) and (36), $\mathcal{OP}_2$ is still a nonconvex optimization problem. In the following section, we propose a successive convex approximation technique to convert $\mathcal{OP}_2$ to a series of convex optimization problems, whose solutions are guaranteed to converge to a suboptimal solution of $\mathcal{OP}_2$.

B. Successive Convex Optimization

The key step of the proposed successive convex optimization approach is to approximate the nonconvex constraints in (35) and (36) with convex bounds at a feasible point. Then, we formulate an approximate convex optimization problem that can be solved efficiently in an iterative manner. The optimal solution of such an approximate convex optimization problem is guaranteed to be a feasible point of the original nonconvex optimization problem [29].

In the following, we explain the convex approximation of the constraint in (35) in detail, and then (36) can be treated similarly. Let $\{\boldsymbol{p}^{(\kappa)}_g, \lambda^{(\kappa)}\}$ be the decision variables of the κth iteration of the optimization problem in $\mathcal{OP}_2$. Then, we can rewrite (35) as follows:

$$\frac{1}{\lambda^{(\kappa)}+3}\left\|\hat{\boldsymbol{\mu}}_{\boldsymbol{g}} + \hat{\boldsymbol{\mu}}_{\boldsymbol{g'}}\right\|^2 \ge \hat{\boldsymbol{\mu}}^T_{\boldsymbol{g}}\hat{\boldsymbol{\mu}}_{g'}. \tag{37}$$

The LHS of the above equation can be further simplified as follows:

$$\begin{aligned}&\frac{\sum_{\ell=1}^{L}\left(M\beta_{g,\ell}p^{(\kappa)}_g + M\beta_{g',\ell}p^{(\kappa)}_{g'} + 2\sigma^2\right)^2}{\lambda^{(\kappa)}+3} \\ &= \frac{\sum_{\ell=1}^{L}\left(\theta^{(\kappa)}_{g,g',\ell}\right)^2}{\lambda^{(\kappa)}+3}\end{aligned} \tag{38}$$

where

$$\theta^{(\kappa)}_{g,g',\ell} = M\beta_{g,\ell}p^{(\kappa)}_g + M\beta_{g',\ell}p^{(\kappa)}_{g'} + 2\sigma^2. \tag{39}$$

Let $\{\boldsymbol{p}^{(\kappa-1)}_g, \lambda^{(\kappa-1)}\}$ be a feasible point to $\mathcal{OP}_2$ that can be found from solving the previous iteration of the optimization problem. Then, with the help of the following inequality:

$$\frac{x^2}{y} \ge \frac{2\bar{x}}{\bar{y}}x - \frac{\bar{x}^2}{\bar{y}^2}y \quad \forall x, \bar{x}, y, \bar{y} > 0 \tag{40}$$

we can show that

$$\frac{\left(\theta^{(\kappa)}_{g,g',\ell}\right)^2}{\lambda^{(\kappa)}} \ge \frac{2\theta^{(\kappa-1)}_{g,g',\ell}}{\lambda^{(\kappa-1)}}\theta^{(\kappa)}_{g,g',\ell} - \frac{\left(\theta^{(\kappa-1)}_{g,g',\ell}\right)^2}{\left(\lambda^{(\kappa-1)}\right)^2}\lambda^{(\kappa)}. \tag{41}$$

The RHS of (37) can be rewritten as follows:

$$\begin{aligned}&p^{(\kappa)}_g p^{(\kappa)}_{g'}\sum_{\ell=1}^{L} M^2\beta_{g,\ell}\beta_{g',\ell} \\ &\quad + \sum_{\ell=1}^{L}\sigma\left(M\beta_{g,\ell}p^{(\kappa)}_g + M\beta_{g',\ell}p^{(\kappa)}_{g'} + \sigma\right).\end{aligned} \tag{42}$$

Using the inequality

$$xy \le \frac{\bar{x}\bar{y}}{4}\left(\frac{x}{\bar{x}} + \frac{y}{\bar{y}}\right)^2 \tag{43}$$

a lower bound of (42) is

$$\begin{aligned}&\frac{p^{(\kappa-1)}_g p^{(\kappa-1)}_{g'}}{4}\left(\frac{p^{(\kappa)}_g}{p^{(\kappa-1)}_g} + \frac{p^{(\kappa)}_{g'}}{p^{(\kappa-1)}_{g'}}\right)^2\sum_{\ell=1}^{L} M^2\beta_{g,\ell}\beta_{g',\ell} \\ &\quad + \sum_{\ell=1}^{L}\sigma\left(M\beta_{g,\ell}p^{(\kappa)}_g + M\beta_{g',\ell}p^{(\kappa)}_{g'} + \sigma\right), 0 < g < g'.\end{aligned} \tag{44}$$

Finally, by substituting (41) and (44) in (37), the nonconvex constraint in (35) is approximated as follows:

$$\sum_{\ell=1}^{L}\left(\frac{2\theta_{g,g',\ell}^{(\kappa-1)}}{\lambda^{(\kappa-1)}}\theta_{g,g',\ell}^{(\kappa)}-\frac{\left(\theta_{g,g',\ell}^{(\kappa-1)}\right)^2}{\left(\lambda^{(\kappa-1)}\right)^2}\lambda^{(\kappa)}\right) \geq \frac{p_g^{(\kappa-1)}p_{g'}^{(\kappa-1)}}{4}\left(\frac{p_g^{(\kappa)}}{p_g^{(\kappa-1)}}+\frac{p_{g'}^{(\kappa)}}{p_{g'}^{(\kappa-1)}}\right)^2\sum_{\ell=1}^{L}M^2\beta_{g,\ell}\beta_{g',\ell} + \sum_{\ell=1}^{L}\sigma\left(M\beta_{g,\ell}p_g^{(\kappa)}+M\beta_{g',\ell}p_{g'}^{(\kappa)}+\sigma\right), 0<g<g'. \quad (45)$$

Similarly, (36) can be approximated as follows:

$$\sum_{\ell=1}^{L}\left(\frac{2\theta_{g,g',\ell}^{(2,\kappa-1)}}{\lambda^{(\kappa-1)}}\theta_{g,g',\ell}^{(2,\kappa)}-\frac{\left(\theta_{g,g',\ell}^{(2,\kappa-1)}\right)^2}{\left(\lambda^{(\kappa-1)}\right)^2}\lambda^{(\kappa)}\right) \geq \frac{p_g^{(\kappa-1)}p_{g'}^{(\kappa-1)}}{4}\left(\frac{p_g^{(\kappa)}}{p_g^{(\kappa-1)}}+\frac{p_{g'}^{(\kappa)}}{p_{g'}^{(\kappa-1)}}\right)^2\sum_{\ell=1}^{L}M^2\beta_{g,\ell}\beta_{g',\ell} + \sum_{\ell=1}^{L}\sigma\left(M\beta_{g,\ell}p_g^{(\kappa)}+M\beta_{g',\ell}p_{g'}^{(\kappa)}+\sigma\right), 0<g<g' \quad (46)$$

where

$$\theta_{g,g',\ell}^{(2,\kappa)}=\left(M\beta_{g,\ell}p_g^{(\kappa)}+M\beta_{g',\ell}p_{g'}^{(\kappa)}+2\sigma^2\right). \quad (47)$$

Remark 1: Given the large number of possible chirps, $M=2^{\mathrm{SF}}$, in a practical LoRa network, the probability of having N_u EDs transmit N_u different chirps is significantly higher than the probability of having less than N_u chirps transmitted by N_u EDs. As such, jointly optimizing $J_{g,g'}$ and $J_{g,g'}^{(2)}$ with equal weights is not likely the best optimization strategy, and we should prioritize the optimization of $J_{g,g'}$ over the optimization of $J_{g,g'}^{(2)}$. This can be done by scaling $\theta_{g,g',\ell}^{(2,\kappa)}$ with a constant α, $\alpha>1$, i.e.,

$$\theta_{g,g',\ell}^{(2,\kappa)}=\alpha\left(M\beta_{g,\ell}p_g^{(\kappa)}+M\beta_{g',\ell}p_{g'}^{(\kappa)}+2\sigma^2\right). \quad (48)$$

Hence, starting with a feasible point $\{\boldsymbol{p}_g^{(\kappa-1)},\lambda^{(\kappa-1)}\}$, the κth instance of the optimization problem $\mathcal{OP}_2$ is modified to

$$\mathcal{OP}_3^{(\kappa)}: \max_{p_g^{(\kappa)},\lambda^{(\kappa)}} \quad \lambda$$
$$\text{subject to (33), (34), (45), (46), (39), (48).}$$

By solving the κth instance of the convex optimization problem $\mathcal{OP}_3^{(\kappa)}$ using convex optimization tools, e.g., CVX [30], we find an optimal solution $\{\boldsymbol{p}_g^{(\kappa)},\lambda^{(\kappa)}\}$ to $\mathcal{OP}_3^{(\kappa)}$ which is also a feasible point to the nonconvex problem in $\mathcal{OP}_2$. The process repeats until convergence. The sequence of feasible points $\{\boldsymbol{p}_g^{(\kappa)},\lambda^{(\kappa)}\}$ is guaranteed to improve the objective function of $\mathcal{OP}_2$ and will eventually converge to a local optimum point that satisfies the KKT conditions [29], [31].

The proposed noncoherent suboptimal detection algorithm is summarized in Algorithm 1.

Algorithm 1 Proposed Power Control and Two-Stage MUD

Require: Large scale fading coefficients $\beta_{g,\ell}$, $p_{\max}$, and ξ.
1: $\kappa=1$. {P}ower control phase (offline)
2: Initially set $p_g^{(\kappa-1)}=p_{\max}$, $\forall g$.
3: **while** Until convergence **do**
4: Approximate constraints (45) and (46) at $p_g^{(\kappa-1)}$.
5: Solve $\mathcal{OP}_3^{(\kappa)}$.
6: Obtain new $p_g^{(k)}$, $\forall g$.
7: **end while**
8: **return** $p_g^{(k)}$.
9: Calculate P_{th} with Golden search based on (28).
10: Identify set of active bins $\mathcal{S}_+$. {T}wo-stage detection phase
11: Build set $\mathcal{S}_d$ of all N_u-tuples based on $\mathcal{S}_+$.
12: Calculating the likelihood of all candidates in $\mathcal{S}_d$ using (30).
13: Choose the candidate with the maximum likelihood as $\hat{\boldsymbol{m}}$.
14: **return** $\hat{\boldsymbol{m}}$.

C. Complexity Analysis

In this section, we present a complexity analysis of the proposed detection algorithms with power control. The power control is done offline and requires the calculations of parameters μ_g and σ_g, $g=1,\ldots,N_u$ as in (17) and (18), respectively, with a complexity order of $\mathcal{O}(2LN_u)$. The power control (steps 3 to 7 in Algorithm 1) solves a convex quadratic programming, which is formulated as a second-order cone programming over N_u+1 variables and $3N_u+\binom{N_u}{2}$ constraints, for every iteration. Hence, the computational complexity of the power control is $\mathcal{O}(N_{\mathrm{iter}}\sqrt{3N_u+\binom{N_u}{2}}(3N_u+2\binom{N_u}{2}))N_u^2)$ [32], where N_{iter} denotes the maximum number of iterations needed for convergence. The offline threshold identification (step 9 in Algorithm 1) solves (28) using the Golden search which has a complexity of $\mathcal{O}(1/\epsilon)$ to obtain an ϵ-accurate solution [33]. The evaluation of (28) requires calculating (22) and (24) with complexity orders of $\mathcal{O}(N_u((M-N_u)N_tL+N_u-1))$ and $\mathcal{O}(LN_tN_uM)$, respectively. Since $M\gg N_u$, the complexity of (22) can be approximated as $\mathcal{O}(LN_tN_uM)$, which is the same as the complexity of (24). Hence, the complexity of the offline threshold identification is $\mathcal{O}(LN_tN_uM/\epsilon)$. It is worth to emphasize that both the power control and threshold identification are processed offline and the results are stored at the network server for long-term usage, and hence, their complexities are not a major concern.

Both the optimal and the suboptimal detection algorithms require calculating $r_{l,k}$ for all L antennas and M frequency bins with the help of the M-point DFT. This requires $\mathcal{O}(LM\log_2 M)$ operations [14]. Then, to calculate the likelihood of the optimal noncoherent ML detection in (12), we need $\mathcal{O}(LM\log_2 M)$ operations for each of M^{N_u} possible N_u-tuples. Thus, the total complexity of the optimal ML detection plus the DFT is $\mathcal{O}(LM^{N_u+1}\log_2 M)$, which is clearly prohibitive for practical LoRa networks. On the other hand, the complexity of the online two-stage suboptimal detection algorithm is analyzed as follows. For the first stage of bin identification (step 10 in Algorithm 1), the complexity of identifying the active bins is $\mathcal{O}(M)$. For the second stage (steps 11 to 13 in Algorithm 1), calculating the likelihood functions of at most $N_u^{N_u}$ candidates requires $\mathcal{O}(LN_u^{N_u+1})$ operations. Hence, the overall complexity of the two-stage suboptimal detection algorithm is at most

TABLE I
SIMULATION PARAMETERS

Parameter	Value
GW height	70 m
ED-GW minimum distance	50 m
ED-ED minimum distance	500 m
Bandwidth	125 kHz
Spreading factor	7
Shadowing standard deviation	7.8 dB
Noise figure	6 dB

$\mathcal{O}(LM\log_2 M(M+LN_u^{N_u+1}))$, which is practically linear in both the number of chirps and the number of GWs.

VI. SIMULATION RESULTS

In this section, we evaluate the performance of the proposed system model and MUD algorithms in terms of the SER. We consider a LoRa network with $L = 3$ GWs simultaneously serving EDs that are randomly located inside a circle having a radius of 4 km. The GWs are equally spaced on a circle of 2-km radius from the center of the coverage area. To make the locations of EDs distinguishable, the minimum distance between any two EDs in a group is set to be 500 m. We consider Rayleigh fading channels with the large-scale fading coefficient calculated for the non-light-of-sight in-car model as in [34]. Specifically, $\beta_{g,\ell} = 128.95 + 23.2\log_{10} d_{g,\ell} + z_{g,\ell}$ dB, where $d_{g,\ell}$ is the distance (in kilometers) from the gth ED to the ℓth GW, and $z_{g,\ell}$ represents shadow fading. In all simulation scenarios, α is set to 1.061, except for Fig. 8, where we examine the impact of α on the system's performance. Other simulation parameters are summarized in Table I.

The SER performance of the proposed LoRa network having multiple EDs in a group transmitting in the same time slot is investigated and compared to that of a conventional LoRa network in which a single ED communicates with a multiple-antenna GW in its own time slot [14]. In order to have a meaningful comparison between the two network models (single ED versus concurrent multiple EDs), a constraint is applied to the sum power of multiple EDs that are grouped for concurrent transmission. In detail, the transmit power $p_g^{(\mathrm{SU})}$ of each ED in the proposed network model required to achieve a predetermined SNR (called a reference SNR) at the closest GW is calculated. Then, the sum transmit power of the grouped EDs is constrained as follows:

$$\sum_{g=1}^{N_u} p_g \le \sum_{g=1}^{N_u} p_g^{(\mathrm{SU})}. \tag{49}$$

On the other hand, from the reference SNR value, the SER in the case of single ED transmission can be theoretically calculated as in [14] when the optimal noncoherent detector is used. In this way, the difference in the SER between the two network models can be observed at the same value of reference SNR.

First, to show the importance of power control in the proposed network model, Fig. 2 plots the SERs obtained with the proposed suboptimal detection algorithm when $N_u = 3$ EDs are grouped for concurrent transmission in the same time slot, and with and without power control. As can be seen, without power control, the SER is very high. As discussed before, the reason for this is that the differences among the EDs' expected power levels are small and the GWs cannot distinguish them despite increasing the number of antennas. On the contrary, with power control, a much better performance is achieved for the same total sum power. Because of the importance of power control, all the remaining results in this section are obtained with power control.

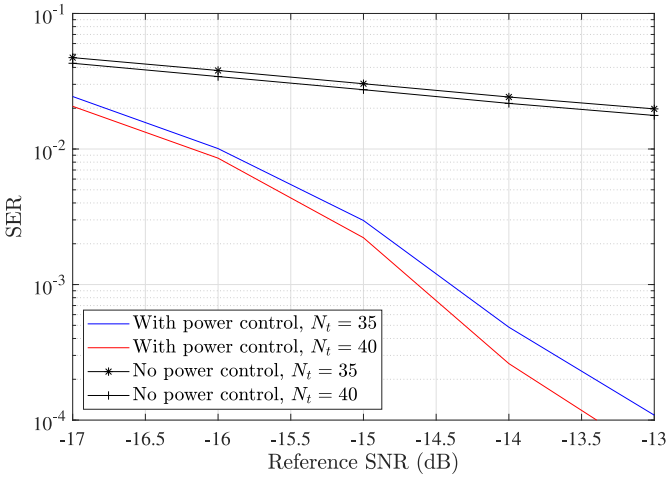

Fig. 2. Effect of power control on SER for $N_u = 3$ EDs in each group, with $N_t = 35$ and $N_t = 40$.

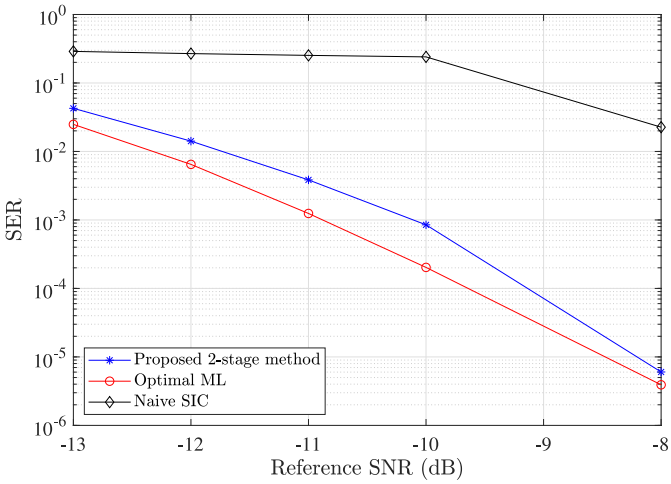

Fig. 3. Performance comparison among the proposed suboptimal 2-stage detection, the optimal ML detection, and a simple MUD: $N_u = 2$, SF $= 5$, and $N_t = 35$.

Fig. 3 compares the performance of the proposed two-stage suboptimal detection algorithm with that of two baseline detection schemes: 1) the optimal ML MUD [see (12)] and 2) a simple MUD method inspired by the successive interference cancelation (SIC) receiver in classical CDMA systems [22]. The comparison is carried out for $N_u = 2$, SF $= 5$, and $N_t = 35$. Note that these parameters' values are chosen to enable the implementation of the ML detection. As pointed out before, with SF values of 7 to 12 in a practical LoRa network, the complexity of the ML detection is simply prohibitive.

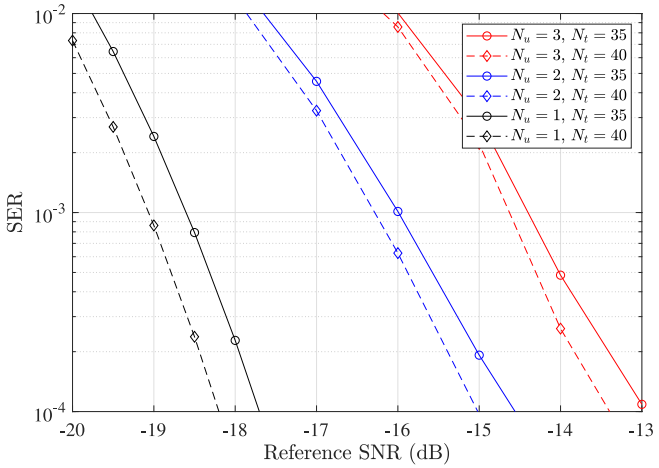

Fig. 4. Average SER versus reference SNR for different numbers of EDs in each group: $N_t = 35$ and $N_t = 40$.

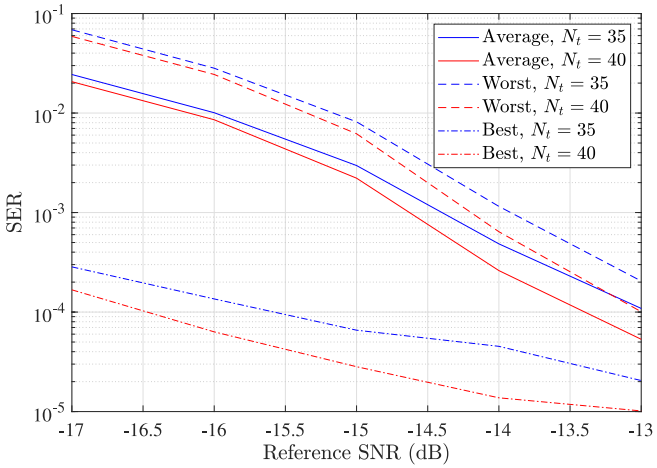

Fig. 5. Best, average, and worst SERs versus reference SNR for $N_u = 3$ EDs in each group: $N_t = 35$ and $N_t = 40$.

For the LoRa system studied in this article, the SIC detection method works as follows. The receiver ignores the multiple access (inter-user) interference and detects the signals of EDs in a sequential manner, i.e., one by one. After the signal of a particular ED has already been detected, it will be subtracted from the superimposed received signals of all EDs, which helps to reduce the interference when detecting the signals for subsequent EDs. Obviously, this interference removal is only helpful when the signals of the preceding EDs are accurately detected. Otherwise, subtracting the incorrectly detected signals can actually introduce more interference that deteriorates the SER. As can be seen from Fig. 3, such a naive SIC detection method performs very poorly in the considered LoRa system, even for the case $N_u = 2$ (two devices are grouped for concurrent transmission). On the other hand, one can see from Fig. 3 that the proposed suboptimal detection algorithm works very well and performs within 1 dB of the optimal ML detection. This clearly demonstrates the usefulness and effectiveness of the proposed suboptimal detection in balancing detection performance and computational complexity.

Fig. 4 plots the average SER curves versus the reference SNR of the proposed network model for the cases of $N_u = 2$ and $N_u = 3$ and for two different sizes of the antenna array at each GW, namely, $N_t = 35$ and $N_t = 40$. Also plotted in the figures are the SER curves of the conventional network model with single ED transmission in each time slot. It can be seen that, for both cases of $N_t = 35$ and $N_t = 40$ antennas at each GW, in order to achieve a SER level of 10^{-4}, the proposed multiuser LoRa networks implemented with $N_u = 2$ and $N_u = 3$ EDs transmitting concurrently in the same time slot require about 3.0 and 4.7 dB more in the transmit power, respectively.

It is important to interpret the above extra transmit power consumption (or equivalently, energy consumption)[2] of the devices properly. In the conventional LoRa network, each ED sends over its own time slot (i.e., $N_u = 1$) in order to avoid collision. In practice, collision avoidance is facilitated by imposing a maximum duty cycle of 1% for all EDs. Depending on the propagation environment (e.g., urban or rural), and the required coverage probability, the total number of EDs that can be served in a conventional LoRa network can be as high as 3000 devices as shown in [35] for an urban environment and coverage probability ≥ 0.9. This means that, with our proposed system model, the total number of EDs can potentially be increased to 6000 and 9000 EDs with $N_u = 2$ and $N_u = 3$, respectively. Given that the overall network capacity can be doubled or tripled by grouping and letting two or three EDs transmit concurrently and detecting their information jointly, the transmit power penalties of 3.0 and 4.7 dB for $N_u = 2$ and $N_u = 3$, respectively, can be well justified for many IoT applications. Moreover, it is pointed out that there are three types of EDs in LoRaWAN: 1) class-A; 2) class-B; and 3) class-C [2]. Class-A and class-B EDs are often battery-powered and expected to have low power/energy consumption. On the other hand, class-C devices are plugged-in [2] and hence their energy consumption is not a major concern. Therefore, class-C devices would benefit the most from our proposed multiuser LoRa networks.

Considering the case $N_u = 3$, Fig. 5 plots the SER of the ED with the highest SER among all three EDs in the group (denoted as the worst ED), the SER of the ED with the lowest SER (denoted as the best ED), and the average SER for all three EDs. It can be seen that, for both $N_t = 35$ and $N_t = 40$, the difference between the SER of the worst ED and the average SER is quite small, while the best ED enjoys a far better performance as compared to the average performance.

Fig. 6 shows the effect of increasing the number of antennas at each GW on the average SER performance. As expected, for both cases of grouping $N_u = 2$ and $N_u = 3$ EDs in the proposed LoRa network model, increasing the number of antennas can significantly improve the SER performance.

The effect of the number of received antennas on the SER can also be observed in Fig. 7 where the average SER is plotted versus the reference SNR. It can be clearly seen that increasing the number of receive antennas helps to reduce the performance gap between the multiuser and single-user scenarios. This is because in the multiuser scenario, not only does

[2]Note that the energy consumption by each ED for sending one information bit (i.e., the energy per bit) equals the product of power consumption and the bit duration (i.e., inverse of the transmission bit rate).

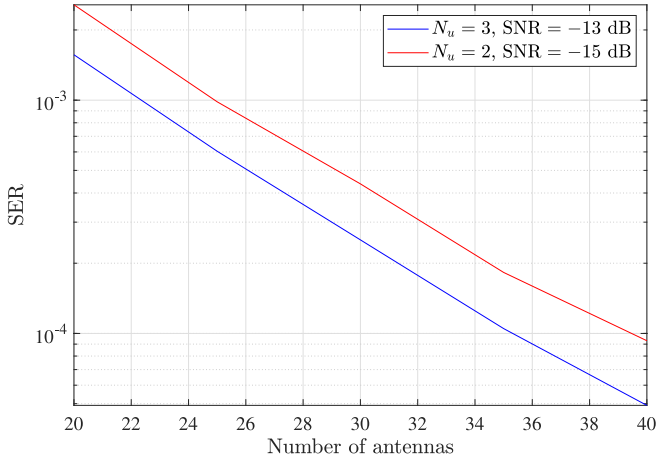

Fig. 6. Effect of the number of antennas at each GW for different values of N_u and reference SNR.

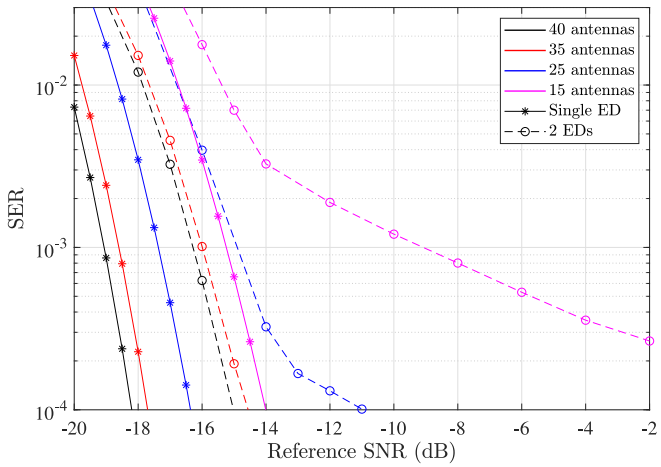

Fig. 7. Average SER versus reference SNR for different numbers of antennas: $N_u = 2$ EDs.

using a larger number of antennas provide a higher diversity gain (as in the single-user scenario), but it also makes the *channel hardening* effect stronger [27] as indicated in (8). Because of this effect, the GWs can distinguish the superimposed signals from different users more effectively based on their unique received power "signatures" (which are related to the transmit powers and user locations). Based on the results in Fig. 7, using $N_t = 35$ antennas appears to be a good choice since further increasing the number of receiver antennas beyond this value does not bring much more performance improvement.

As discussed earlier, the proper selection of α for prioritizing $J_{g,g'}$ over $J^{(2)}_{g,g'}$ in $\mathcal{OP}_3^{(\kappa)}$ is necessary to balance the detection performance. In particular, as the value of α increases, minimizing $J_{g,g'}$ is prioritized over the minimization of $J^{(2)}_{g,g'}$. Fig. 8 shows the effect of α on the SER performance for the proposed LoRa network model with $N_u = 3$, $N_t = 40$ antennas, and SNR $= -13$ dB. As can be seen, the SER improves (i.e., decreases) when α increases from 1 to 1.06, which agrees with our observation that the detection error when 2 or more EDs transmitting the same chirp decreases. The SER performance then deteriorates when increasing α beyond 1.06.

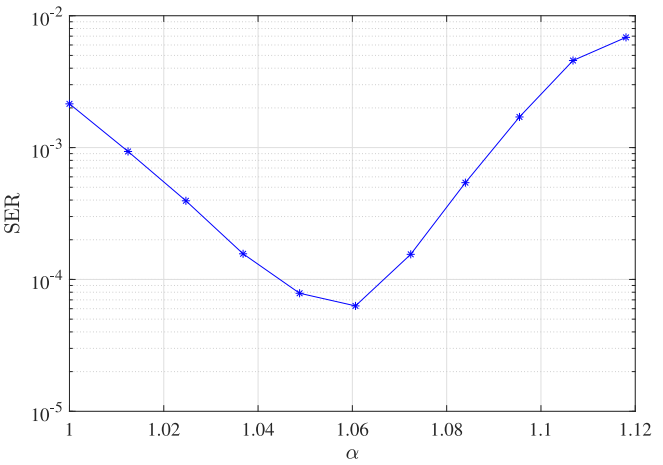

Fig. 8. SER versus α with $N_u = 3$ EDs in each group, $N_t = 40$ antennas, and reference SNR $= -13$ dB.

VII. Conclusion

In this article, we have proposed and investigated the performance of a novel LoRa network model by grouping and allowing multiple EDs to simultaneously transmit information to GWs using the same SF factor and over the same frequency band. By exploiting large antenna arrays at GWs, we developed both the optimal ML detection and two-stage suboptimal detection algorithms to jointly detect information bits of multiple EDs. The proposed suboptimal two-stage detection algorithm identifies the active frequency bins in the first stage and jointly detects the symbols of EDs in the second stage. A power control policy was also proposed to improve the detection performance in the second stage by minimizing the similarity, measured by the Jaccard coefficient, among expected bin powers between any pairs of EDs in the group. The solution of the power control problem is obtained via successive convex approximation. Simulation results showed the merits of the proposed network model, the importance of power control, and the effectiveness of the two-stage suboptimal detection algorithm. More importantly, the results demonstrate and justify the tradeoff between transmit power penalties and network scalability of the proposed network model. In particular, by grouping and allowing concurrent transmission of two or three EDs in the same time slot, the uplink capacity of the proposed network can be doubled or tripled over that of a conventional LoRa network at the expense of additional 3.0 or 4.7 dB transmit power.

References

[1] K. Figueredo, D. Seed, and V. Subotic, "Preparing for highly scalable and replicable IoT systems," *IEEE Internet Things Mag.*, vol. 3, no. 3, pp. 94–98, Sep. 2020.

[2] M. Centenaro, L. Vangelista, A. Zanella, and M. Zorzi, "Long-range communications in unlicensed bands: The rising stars in the IoT and smart city scenarios," *IEEE Trans. Wireless Commun.*, vol. 23, no. 5, pp. 60–67, Oct. 2016.

[3] O. Afisiadis, M. Cotting, A. Burg, and A. Balatsoukas-Stimming, "On the error rate of the LoRa modulation with interference," *IEEE Trans. Wireless Commun.*, vol. 19, no. 2, pp. 1292–1304, Nov. 2019.

[4] A. Mahmood, E. Sisinni, L. Guntupalli, R. Rondón, S. A. Hassan, and M. Gidlund, "Scalability analysis of a LoRa network under imperfect orthogonality," *IEEE Trans. Ind. Informat.*, vol. 15, no. 3, pp. 1425–1436, Mar. 2019.

[5] M. Hanif and H. H. Nguyen, "Methods for improving flexibility and data rates of chirp spread spectrum systems in LoRaWAN," U.S. Patent 10 778 282, Sep. 2020.
[6] M. Hanif and H. H. Nguyen, "Frequency-shift chirp spread spectrum communications with index modulation," *IEEE Internet Things J.*, vol. 8, no. 24, pp. 17611–17621, Dec. 2021.
[7] T. Elshabrawy and J. Robert, "Closed-form approximation of LoRa modulation BER performance," *IEEE Commun. Lett.*, vol. 22, no. 9, pp. 1778–1781, Sep. 2018.
[8] M. Hanif and H. H. Nguyen, "Slope-shift keying LoRa-based modulation," *IEEE Internet Things J.*, vol. 8, no. 1, pp. 211–221, Jan. 2021.
[9] T. T. Nguyen, H. H. Nguyen, R. Barton, and P. Grossetete, "Efficient design of chirp spread spectrum modulation for low-power wide-area networks," *IEEE Internet Things J.*, vol. 6, no. 6, pp. 9503–9515, Dec. 2019.
[10] T. Elshabrawy and J. Robert, "Interleaved chirp spreading LoRa-based modulation," *IEEE Internet Things J.*, vol. 6, no. 2, pp. 3855–3863, Apr. 2019.
[11] R. Bomfin, M. Chafii, and G. Fettweis, "A novel modulation for IoT: PSK-LoRa," in *Proc. IEEE Veh. Technol. Conf.*, Apr. 2019, pp. 1–5.
[12] A. W. Azim, J. L. G. Monsalve, and M. Chafii, "Enhanced PSK-LoRa," *IEEE Wireless Commun. Lett.*, vol. 11, no. 3, pp. 612–616, Mar. 2022.
[13] G. Baruffa and R. Luca, "Performance of LoRa-based schemes and quadrature chirp index modulation," *IEEE Internet Things J.*, vol. 9, no. 10, pp. 7759–7772, May 2022.
[14] K. Nguyen, H. H. Nguyen, and E. Bedeer, "Performance improvement of LoRa modulation with signal combining and semi-coherent detection," *IEEE Commun. Lett.*, vol. 25, no. 9, pp. 2889–2893, Sep. 2021.
[15] J. Xu, P. Zhang, S. Zhong, and L. Huang, "Discrete particle swarm optimization based antenna selection for MIMO LoRa IoT systems," in *Proc. Comput. Commun. IoT Appl. (ComComAp)*, Oct. 2019, pp. 204–209.
[16] A. A. Tesfay, E. P. Simon, I. Nevat, and L. Clavier, "Multiuser detection for downlink communication in LoRa-like networks," *IEEE Access*, vol. 8, pp. 199001–199015, 2020.
[17] L. Beltramelli, A. Mahmood, P. Österberg, and M. Gidlund, "LoRa beyond ALOHA: An investigation of alternative random access protocols," *IEEE Trans. Ind. Informat.*, vol. 17, no. 5, pp. 3544–3554, May 2021.
[18] M. Luvisotto, F. Tramarin, L. Vangelista, and S. Vitturi, "On the use of LoRaWAN for indoor industrial IoT applications," *Wireless Commun. Mobile Comput.*, vol. 2018, May 2018, Art. no. 3982646.
[19] J. Haxhibeqiri, A. Karaagac, F. Van den Abeele, W. Joseph, I. Moerman, and J. Hoebeke, "LoRa indoor coverage and performance in an industrial environment: Case study," in *Proc. IEEE Int. Conf. Emerg. Technol. Factory Autom. (ETFA)*, Sep. 2017, pp. 1–8.
[20] J. Haxhibeqiri, I. Moerman, and J. Hoebeke, "Low overhead scheduling of LoRa transmissions for improved scalability," *IEEE Internet Things J.*, vol. 6, no. 2, pp. 3097–3109, Apr. 2019.
[21] B. Reynders, Q. Wang, P. Tuset-Peiro, X. Vilajosana, and S. Pollin, "Improving reliability and scalability of LoRaWANs through lightweight scheduling," *IEEE Internet Things J.*, vol. 5, no. 3, pp. 1830–1842, Jun. 2018.
[22] S. Verdu, *Multiuser Detection*. Cambridge, U.K.: Cambridge Univ. Press, 1998.
[23] S. Verdu, "Minimum probability of error for asynchronous Gaussian multiple-access channels," *IEEE Trans. Inf. Theory*, vol. IT-32, no. 1, pp. 85–96, Jan. 1986.
[24] S. Moshavi, "Multi-user detection for DS-CDMA communications," *IEEE Commun. Mag.*, vol. 34, no. 10, pp. 124–136, Oct. 1996.
[25] A. Duel-Hallen, J. Holtzman, and Z. Zvonar, "Multiuser detection for CDMA systems," *IEEE Pers. Commun.*, vol. 2, no. 2, pp. 46–58, Apr. 1995.
[26] R. Ghanaatian, O. Afisiadis, M. Cotting, and A. Burg, "LoRa digital receiver analysis and implementation," in *Proc. IEEE Int. Conf. Acoust. Speech Signal Process. (ICASSP)*, May 2019, pp. 1498–1502.
[27] T. L. Marzetta and H. Q. Ngo, *Fundamentals of Massive MIMO*. Cambridge, U.K.: Cambridge Univ. Press, 2016.
[28] S.-H. Cha, "Comprehensive survey on distance/similarity measures between probability density functions," *Int. J. Math. Models Methods Appl. Sci.*, vol. 1, no. 4, pp. 300–307, Nov. 2007.
[29] S. Boyd and L. Vandenberghe, *Convex Optimization*. Cambridge, U.K.: Cambridge Univ. Press, 2004.
[30] M. Grant and S. Boyd. "CVX: MATLAB software for disciplined convex programming." 2010. [Online]. Available: https://cvxr.com/cvx
[31] T. K. Nguyen, H. H. Nguyen, and H. D. Tuan, "Max–min QoS power control in generalized cell-free massive MIMO-NOMA with optimal backhaul combining," *IEEE Trans. Veh. Technol.*, vol. 69, no. 10, pp. 10949–10964, Oct. 2020.
[32] M. S. Lobo, L. Vandenberghe, S. Boyd, and H. Lebret, "Applications of second-order cone programming," *Linear Algebra Appl.*, vol. 284, nos. 1–3, pp. 193–228, 1998.
[33] D. G. Luenberger and Y. Ye, *Linear and Nonlinear Programming*. Cham, Switzerland: Springer, 1984.
[34] J. Petajajarvi, K. Mikhaylov, A. Roivainen, T. Hanninen, and M. Pettissalo, "On the coverage of LPWANs: range evaluation and channel attenuation model for LoRa technology," in *Proc. IEEE Int. Conf. ITS Telecommun. (ITST)*, Dec. 2015, pp. 55–59.
[35] P. Edward, M. El-Aasser, M. Ashour, and T. Elshabrawy, "Interleaved chirp spreading LoRa as a parallel network to enhance LoRa capacity," *IEEE Internet Things J.*, vol. 8, no. 5, pp. 3864–3874, Mar. 2021.

The Khai Nguyen received the B.Eng. degree from the School of Electronics and Telecommunications, Hanoi University of Science and Technology, Hanoi, Vietnam, in 2017, and the M.Sc. degree in electrical engineering from the University of Saskatchewan, Saskatoon, SK, Canada, in 2020, where he is currently pursuing the Ph.D. degree.

His research fields include wireless communication, channel coding, and signal processing for broadband systems.

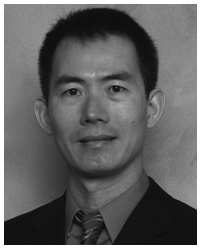

Ha H. Nguyen (Senior Member, IEEE) received the bachelor's degree in electrical engineering from Hanoi University of Technology, Hanoi, Vietnam, in 1995, the master's degree in electrical engineering from the Asian Institute of Technology, Bangkok, Thailand, in 1997, and the Ph.D. degree in electrical engineering from the University of Manitoba, Winnipeg, MB, Canada, in 2001.

He joined the Department of Electrical and Computer Engineering, University of Saskatchewan, Saskatoon, SK, Canada, in 2001, and became a Full Professor in 2007. He currently holds the position of NSERC/Cisco Industrial Research Chair in low-power wireless access for sensor networks. He has coauthored with Ed Shwedyk the textbook *A First Course in Digital Communications* (Cambridge University Press). His research interests span broad areas of communication theory, wireless communications, and statistical signal processing.

Dr. Nguyen was an Associate Editor for the IEEE TRANSACTIONS ON WIRELESS COMMUNICATIONS and IEEE WIRELESS COMMUNICATIONS LETTERS from 2007 to 2011 and from 2011 to 2016, respectively. He is currently serving as an Associate Editor for the IEEE TRANSACTIONS ON VEHICULAR TECHNOLOGY and IEEE TRANSACTIONS ON COMMUNICATIONS. He served as a Technical Program Chair for numerous IEEE events, and was the General Chair for the 30th Biennial Symposium on Communications 2021. He is a Fellow of the Engineering Institute of Canada and a Registered Member of the Association of Professional Engineers and Geoscientists of Saskatchewan.

Ebrahim Bedeer (Member, IEEE) received the B.Sc. (Hons.) and M.Sc. degrees in electrical engineering from Tanta University, Tanta, Egypt, in 2002 and 2008, respectively, and the Ph.D. degree in electrical engineering from Memorial University, St. Johns, NL, Canada, in 2014.

He joined the Department of Electrical and Computer Engineering, University of Saskatchewan, Saskatoon, SK, Canada, in 2019, as an Assistant Professor. Before that, he was an Assistant Professor (a Lecturer in the U.K.) with Ulster University, London, U.K., and a Postdoctoral Fellow with Carleton University, Ottawa, ON, Canada, and The University of British Columbia, Kelowna, BC, Canada. His current research interests include applications of optimization techniques in signal processing and wireless communications, spectral efficient communication systems, and Internet of Things.

Dr. Bedeer is a Registered Member of the Association of Professional Engineers and Geoscientists of Saskatchewan.